Polymer 49 (2008) 5490–5496

Contents lists available at ScienceDirect

Polymer

journal homepage: www.elsevier.com/locate/polymer

pH-induced conformational changes of loosely grafted molecular brushes containing poly(acrylic acid) side chains

Hyung-il Lee [a], Jamie R. Boyce [b], Alper Nese [a], Sergei S. Sheiko [b], Krzysztof Matyjaszewski [a,*]

[a] Center for Macromolecular Engineering, Department of Chemistry, Carnegie Mellon University, 4400 Fifth Avenue, Pittsburgh, PA 15213, USA
[b] Department of Chemistry, University of North Carolina at Chapel Hill, Chapel Hill, NC 27599-3290, USA

ARTICLE INFO

Article history:
Received 13 August 2008
Received in revised form
24 September 2008
Accepted 2 October 2008
Available online 14 October 2008

Keywords:
ATRP
Molecular brushes
Poly(acrylic acid)

ABSTRACT

A series of water-soluble loosely grafted poly(acrylic acid) (PAA) brushes with four different grafting densities were synthesized by the "grafting from" approach using atom transfer radical polymerization (ATRP). Gel permeation chromatography (GPC) and ^{1}H NMR spectroscopy were used to provide evidence for formation of the well-defined backbones and the resulting brush copolymers. Atomic force microscopy was used to study the conformation of adsorbed brushes as a function of pH. The adsorbed molecules undergo a globule-to-extended conformational transition as the solution is changed from acidic to basic. This transition was monitored on a mica surface by imaging individual molecules with atomic force microscopy (AFM). The conformational behavior was compared with 100%-grafted PAA brushes. Unlike the loose brushes, the 100%-grafted molecules remained fully extended in a broad range of pH values (pH = 2–9) due to steric repulsion between the densely grafted side chains which is strongly enhanced upon adsorption to a substrate.

1. Introduction

Recently, the properties and behavior of single polymeric chains, especially molecular bottle brushes, have been studied extensively due to their potential as materials with novel properties, such as supersoft elastomers [1,2] or templates for nanorod or nano particles [3–5]. Bottle brushes are a special type of graft copolymer in which multiple polymer chains are grafted to a polymer backbone. Because of this dense grafting, bottle brushes usually exhibit an extended conformation due to steric repulsion between the densely grafted side chains [6]. This behavior, however, changes when dealing with loosely grafted molecules whose conformation is controlled by long range interactions. This is relevant to proteoglycan brushes that are found in a variety of places within the body, performing many different functions including cell-to-cell signaling, joint lubrication, and cell surface protection [7–12].

They consist of a core protein with loosely grafted glycosaminoglycan chains, which are long, linear carbohydrate polymers that are negatively charged under physiological conditions. It is believed that this brush-like architecture gives proteoglycan molecules their functionality. For example, proteoglycan in the cartilage acts as a water sponge, expelling water and collapsing when pressure is put on the joint, and taking up water and expanding when the pressure is released. This function helps provide the cartilage its important shock-absorbing and lubricious qualities [13–16]. A lack of these molecules within the cartilage has been linked to osteoarthritis. Synthetic substitutes for natural proteoglycans have been proposed in order to better understand the architecture–functionality relationship, which could potentially lead to advances in biomedical applications [17–24].

Controlled/living radical polymerization (CRP) [25–29] provides an easy way to prepare polymers with controlled molecular weight and various architectures. Among them, atom transfer radical polymerization (ATRP) [30,31] is the most efficient method for the synthesis of molecular bottle brushes [32–40]. By using the ATRP technique, brushes with various molecular architectures, such as multi-arm starlike structures [41–44], cylindrical brush–coil block copolymers [45], brushes with block copolymer side chains [46–50] and brushes with a gradient in grafting density along the copolymer backbone [51–53], have been synthesized. Loosely grafted molecular brushes can be also prepared by simple manipulation of the grafting density.

In an effort to propose synthetic substitutes for proteoglycans, we describe preparation of a series of water-soluble loosely grafted brush macromolecules with poly(acrylic acid) (PAA) side chains using the ATRP technique. Molecular conformation on substrate was studied through imaging of single molecules by Atomic Force Microscopy (AFM). Unlike the extended conformation of dense

* Corresponding author. Tel.: +1 412 268 3209; fax: +1 412 268 6897.
E-mail address: km3b@andrew.cmu.edu (K. Matyjaszewski).

0032-3861/$ – see front matter © 2008 Elsevier Ltd. All rights reserved.
doi:10.1016/j.polymer.2008.10.001

brushes, the loosely grafted molecules exhibit a pH-induced conformational transition as a result of their architecture and chemical composition. Because PAA is a weak polyelectrolyte with a $pK_a \sim 6.8$ at high molecular weights, changes in pH result in changes in the degree of protonation, and thus the charge density [54–56]. The competition between the hydrophobic PMMA backbone and the slowly deprotonating PAA side chains results in a gradual globule-to-extended conformational transition from about pH 4 to pH 9.

2. Experimental

2.1. Materials

2-(Trimethylsilyloxy)ethyl methacrylate (HEMATMS) (99%) was purchased from Polysciences. Anisole (99%), methyl methacrylate (MMA) and *t*-butyl acrylate were purchased from Acros and distilled under vacuum prior to use. Ethyl 2-bromoisobutyrate (98%) (EBiB), 2-bromopropionyl bromide (98%), 4,4′-di-(nonyl)-2,2′-bipyridine (dNbpy), potassium fluoride (97%), 1 M tetrabutylammonium fluoride in THF were purchased from Aldrich Chemical Co.

2.2. Equipment and analysis

The apparent molecular weight and molecular weight distributions of the polymers were measured using a GPC system, consisted of a Waters 510 HPLC pump, three Waters UltraStyragel columns (100, 10^3, and 10^5 Å), and a Waters 410 differential refractive index detector, with a THF flow rate of 1.0 mL/min. Poly(methyl methacrylate) (PMMA) was used as a calibration standard employing WinGPC software from Polymer Standards Service. ^{1}H NMR spectra were collected in deuterated chloroform at 30 °C using a Bruker 300 MHz spectrometer. Monomer conversion was determined by gas chromatography (GC) using a Shimadzu GC 14-A gas chromatograph equipped with a FID detector and ValcoBond 30 m VB WAX Megabore column. AFM images were collected using a Multimode Atomic Force Microscope (Veeco Metrology Group) equipped with a Nanoscope IIIa control station in tapping mode. We used Si cantilevers with a resonance frequency of about 140 kHz and a spring constant of about 5 N/m. The radius of the probe was less than 10 nm. To ensure accurate characterization of molecules, multiple images were collected from different areas of the same sample using different scan sizes and scan directions. The image analysis was performed using specially developed software which allows accurate characterization of molecular dimensions and shape. Samples for AFM measurements were spin cast onto mica from 0.05 mg/mL aqueous solutions, the pH of which was altered by the addition of dilute sodium hydroxide or hydrochloric acid. The conformation of adsorbed macromolecules was preserved due to the high glass transition temperature of PAA ($T_g = 103$ °C).

2.3. Synthesis

2.3.1. General procedures

2.3.1.1. Poly(methyl methacrylate-stat-*2-(trimethylsilyloxy)ethyl methacrylate), (PMMA*-stat-*PHEMATMS), (**H1**).* MMA (4.0 g, 40 mmol), HEMATMS (2.02 g, 10 mmol), anisole (2.0 mL), $CuBr_2$ (0.56 mg, 0.0025 mmol), and dNbpy (0.042 g, 0.1 mmol) were added to a 25-mL Schlenk flask and the reaction mixture was degassed by three freeze–pump–thaw cycles. After stirring for 0.5 h at room temperature, CuBr (7.0 mg, 0.05 mmol) was added under nitrogen. An initial sample was taken by syringe, and then the initiator, EBiB (7.34 μL, 0.05 mmol), was added. The flask was placed in a preheated oil bath at 80 °C. The polymerization was stopped after 5 h by cooling the flask to room temperature and opening the flask to air. The resulting polymer solution was purified by passing through a column of neutral alumina and then precipitated into cold methanol. The solid polymer was filtered and dried under high vacuum at room temperature for 24 h. (GPC: $M_n = 68{,}000$ g/mol, $M_w/M_n = 1.20$).

2.3.1.2. Poly(methyl methacrylate-stat-*2-(2-bromopropionyloxy)ethyl methacrylate), (PMMA*-stat-*PBPEM), (**E1**).* A sample of PMMA-*stat*-PHEMATMS, (**H1**) (3.0 g, assuming 5.0 mmol of TMS groups) was placed in a 100 mL round-bottom flask. KF (0.32 g, 5.5 mmol) was added, the flask was sealed and flushed with N_2, and dry THF (50 mL) was added. A 1.0 M solution of tetrabutylammonium fluoride in THF (0.05 mL, 0.05 mmol) was added dropwise to the flask, followed by the slow addition of 2-bromopropionyl bromide (1.62 g, 7.5 mmol) over the course of 15 min. The reaction mixture was stirred overnight at room temperature and precipitated into methanol/cold water (80/20 v/v%). The separated precipitate was redissolved in $CHCl_3$ (30 mL), filtered through a column of basic alumina, and the solvent was removed under vacuum. The isolated polymer was reprecipitated from THF once into MeOH and three times into hexanes, and dried under vacuum at 25 °C for 24 h. (GPC: $M_n = 64{,}000$ g/mol, $M_w/M_n = 1.21$).

2.3.1.3. Poly[methyl methacrylate-stat-*{2-(2-bromopropionyloxy)ethyl methacrylate*-graft-tert-*butyl acrylate}], [PMMA*-stat-*(PBPEM*-graft-*PtBA)], (**B1**).* PMMA-*stat*-PBPEM, (**E1**) (0.05 g, assumed to contain 0.083 mmol of initiating groups), *t*-BA (4.25 g, 33.2 mmol), anisole (0.5 mL) and dNbpy (0.068 mg, 0.166 mmol) were added to a 10-mL Schlenk flask and the reaction mixture was degassed by three freeze–pump–thaw cycles. After stirring for 0.5 h at room temperature, CuBr (0.012 g, 0.083 mmol) was added under nitrogen, and the flask was placed in a preheated oil bath at 70 °C. The polymerization was stopped after 25 h by cooling the flask to room temperature and opening the flask to air. The resulting polymer solution was purified by passing through a column of neutral alumina. Solvent and the remaining monomer were removed under high vacuum (1 mmHg). The resulting product was dried at room temperature for 12 h. (DP_{sc} of *t*-BA = 57, as determined by gravimetry.) (GPC: $M_n = 763{,}000$ g/mol, $M_w/M_n = 1.21$.)

2.3.1.4. Poly[methyl methacrylate-stat-*{2-(2-bromopropionyloxy)ethyl methacrylate*-graft-*acrylic acid}], [PMMA*-stat-*(PBPEM*-graft-*PAA)], (**P1**).* [PMMA-*stat*-(PBPEM-*graft*-PtBA)], (B1) (0.33 g, assumed to contain 2.3 mmol of *t*-BA groups), was dissolved in dichloromethane. A fivefold molar excess of CF_3COOH was added and the reaction mixture was stirred at room temperature for 48 h. The precipitated PAA brush was filtered and washed with THF and dried in the vacuum oven at 50 °C for 24 h.

3. Results and discussion

3.1. Synthesis

The synthetic route for the preparation of loosely grafted PAA copolymer brushes is outlined in Scheme 1. ATRP was used to directly prepare a series of linear PMMA-*s*-PHEMATMS copolymers (**H1**, **H2**, **H3** and **H4**) with controlled molecular weight and low polydispersity. As a point of reference, homo PHEMATMS (**H0**) was also prepared to yield a PAA brush with 100% grafting density (**P0**). By controlling the feed ratio of MMA and HEMATMS, PMMA-*s*-PHEMATMS with four different compositions was prepared (5, 10, 15 and 20% of HEMATMS along the backbone). Since two monomers, MMA and HEMATMS, have similar reactivities, the copolymer composition was the same as comonomer feed ratio with random distribution of the two monomers along the copolymer chain. A CuBr/dNbpy catalyst system was used for the copolymerization of

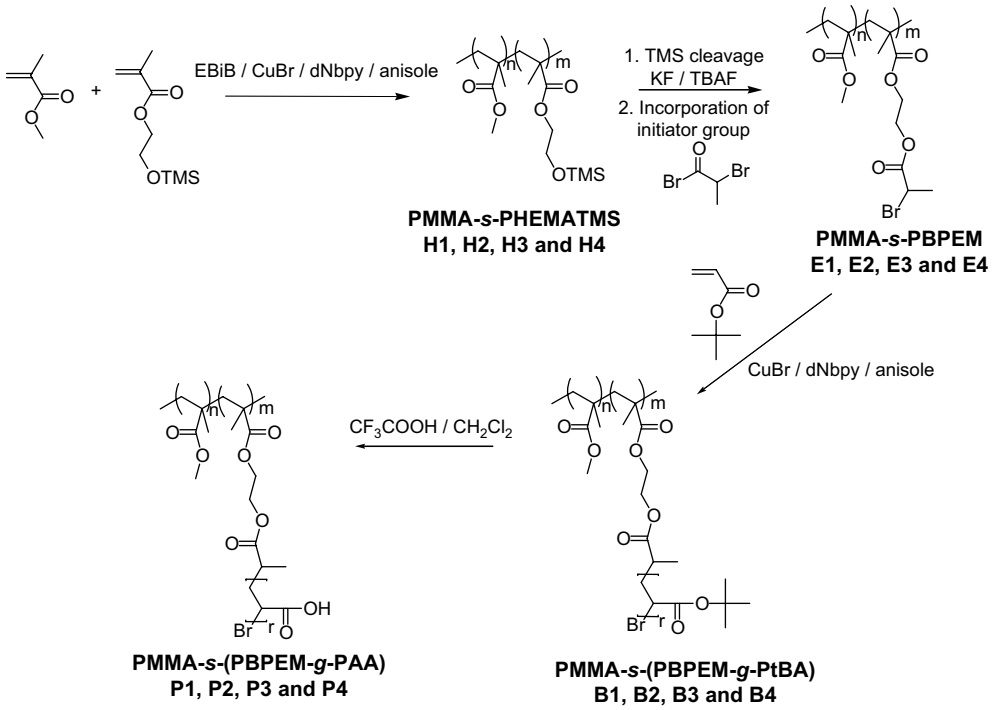

Scheme 1. Synthesis of a molecular brush containing PAA in the side chains from a PMMA-*s*-PBPEM backbone.

MMA and HEMATMS using ethyl 2-bromoisobutyrate (EBiB) as an initiator. During copolymerization of **H1** (monomer feed ratio, MMA:HEMATMS = 80:20), the monomer conversions of MMA and HEMATMS reached 45 and 48% in 5 h, respectively. The resulting copolymer with $M_n = 68{,}000$ g/mol and polydispersity of $M_w/M_n = 1.20$ was obtained by GPC. The reaction conditions and results for the copolymerization of MMA and HEMATMS are summarized in Table 1.

In the next step, bromine-containing ATRP initiating groups in the backbone were introduced by an esterification reaction, which was accomplished by reacting the PMMA-*s*-PHEMATMS with 2-bromopropionyl bromide in situ using potassium fluoride/tetrabutylammonium fluoride in dry THF. A series of isolated macroinitiators (**E0**, **E1**, **E2**, **E3** and **E4**) were characterized by ^{1}H NMR spectroscopy and GPC. The ^{1}H NMR spectra were used to directly determine the fraction of the ATRP initiating groups, PBPEM, along the backbone. In Fig. 2, the peaks b and c at 4.22 and 4.40 ppm represent the methylene protons between two ester groups from PBPEM units, and peak a represents the methoxy protons from PMMA units. The integral ratio between peaks a and c was used to calculate the fraction of PBPEM units in the backbone. The values were close to theoretical results which were determined by monomer conversion obtained from GC. The esterified PMMA-*s*-PBPEM macroinitiators were also characterized by GPC, which was calibrated with PMMA standards. No visible shift in molecular weight was observed as **H1** was transformed to **E1**, as shown in the overlaid GPC traces (Fig. 1) and no significant tailing or shoulder was observed, indicating negligible contributions of side reactions during the esterification reactions.

A series of fully and loosely grafted molecular brushes (**B0**, **B1**, **B2**, **B3** and **B4**) were synthesized by polymerizing *t*-BA from aforementioned macroinitiators (Scheme 1). Data of the M_n and M_w/M_n for the resulting brushes are compiled in Table 2, and the overlaid GPC traces are shown in Fig. 1. The increase in the molecular weight of the graft copolymer **B1** is demonstrated by the complete shift of the GPC trace toward higher molecular weight by comparison with the backbone macroinitiators, and the polydispersity was relatively low. The reaction conditions and results for the resulting loosely grafted PtBA brushes are summarized in Table 2.

Hydrolysis of the PtBA side chains was conducted under relatively mild acidic conditions using CF_3COOH in methylene chloride.

Table 1
Reaction conditions and results for the copolymerization of MMA and HEMATMS.

Backbones	[M]:[H]:[I]:[L]:[Cu$^+$]:[Cu^{++}][a]	Conv[b] (%)		$M_{n,app}$[c] ($\times 10^{-4}$)	PDI[c]	DP				Macroinitiator (%)	
		M	H			GC		NMR[d]		NMR	GC
						M	H	M	H		
H0	–:600:1:2:1:0.05	–	75	7.5	1.16	–	450	–	450	100	100
H1	800:200:1:2:1:0.05	45	48	6.8	1.21	360	96	352	104	22.7	21.1
H2	850:150:1:2:1:0.05	39	39	6.9	1.19	332	59	324	67	17.2	15.1
H3	900:100:1:2:1:0.05	41	46	7.1	1.2	369	46	367	48	11.5	11.1
H4	950:50:1:2:1:0.05	45	50	5.8	1.23	428	25	425	28	6.3	5.5

[a] M = MMA, H = HEMATMS, I = EBiB, L = dNbpy, Cu^+ = CuBr, Cu^{++} = $CuBr_2$.
[b] Obtained from gas chromatography.
[c] Determined by gel permeation chromatography in THF with PMMA calibration.
[d] Calculated from NMR results after transformation of PHEMATMS to PBPEM, based on the total DP of the backbone obtained from GC.

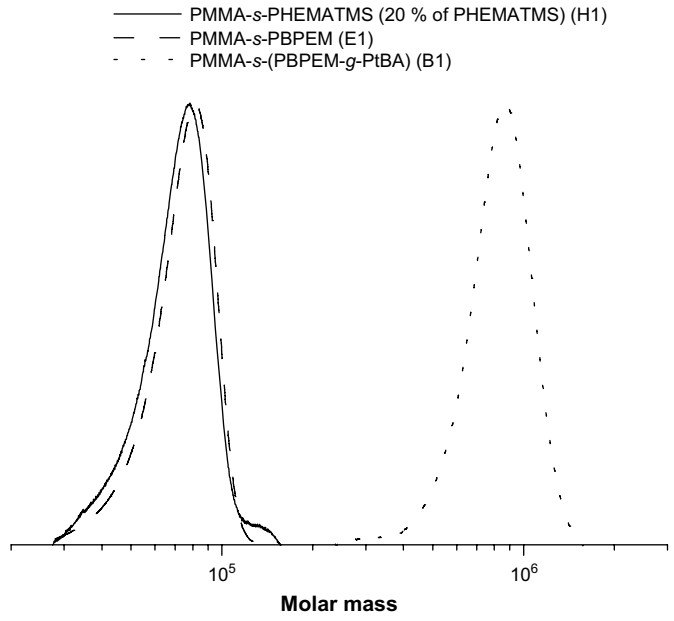

Fig. 1. GPC traces of PMMA-*s*-PHEMATMS (20% of HEMATMS along the backbone) (**H1**), PMMA-*s*-PBPEM (**E1**) and the resulting [PMMA-*s*-(PBPEM-*g*-PtBA)], (**B1**).

The successful hydrolysis of PtBA groups was demonstrated by the disappearance of the methyl protons of the *t*-butyl group peak at 1.45 ppm (Fig. 3). The resulting fully and loosely grafted PAA brushes (**P0**, **P1**, **P2**, **P3** and **P4**) were used to study a pH-induced rod–globule transition.

3.2. AFM analysis of pH-induced conformational transition

AFM is a convenient characterization tool for brush-like macromolecules because it can directly image individual molecules, allowing verification of synthesis as well as determination of molecular conformation on surfaces [57–60]. Fig. 4 demonstrates the extended conformation of fully grafted, i.e. 100% PAA brushes (**P0**). The observed molecular conformation is caused by repulsion of the densely grafted side chains. The side chain crowding is enhanced upon adsorption of the brushes on a substrate which

Table 2
Reaction conditions and results for the synthesis of the molecular brushes containing PtBA in the side chain.

Brushes	Macro-initiators	[M]:[MI]:[L]:[Cu^+]:[Cu^{++}][a]	Conv[b] (%)	$M_{n,app}$[c] ($\times10^{-5}$)	PDI[c]	DP[d]	DP_n[e]
B0	**E0**	400:1:1:0.5:0.025	9	7.8	1.18	34	36
B1	**E1**	400:1:1:0.5:0.025	14	7.6	1.21	57	57
B2	**E2**	400:1:1:0.5:0.025	12	4.2	1.19	47	49
B3	**E3**	400:1:1:0.5:0.025	13	5.0	1.42	53	72
B4	**E4**	400:1:1:0.5:0.025	6	1.7	1.23	24	36

[a] M = *t*-BA, MI = macroinitiators, L = dNbpy, Cu^+ = CuBr, Cu^{++} = $CuBr_2$.
[b] Obtained from gravimetry.
[c] Determined by gel permeation chromatography in THF with PMMA calibration.
[d] Calculated from gravimetry results.
[e] $DP_{n\text{-theory}} = (M_{n,brush} - M_{n,macroinitiator})/(m_0 \times DP_{n,PBPEM})$, where m_0 is the molecular weight of the side chain monomer unit: *t*-butyl acrylate (128 g/mol).

makes the conformation largely independent of the solvent quality. This was confirmed by AFM experiments. The 100%-grafted molecules adsorbed from aqueous solutions in a broad pH range (pH = 2–9) demonstrated a conformation identical to that in Fig. 4. The conformation of densely grafted brushes on a substrate strongly depends on the strength of attraction to the substrate which determines the number of adsorbed side chains [59]. Additional repulsion will not lead to the increase of the contour length of already fully extended backbone, but may cause scission of covalent bonds reported for neutral brush molecules [61].

Different behavior is expected for loosely grafted molecules (<20%). Under good solvent conditions, swollen side chains repel one another and force the backbone to extend. If the solvent quality for the side chains changes, the conformation of the molecule will also change. In addition, using water as a solvent and varying the pH induced dissociation of AA monomeric units, resulting in electrostatic repulsion between negatively charged carboxylic groups. The long range Coulomb interactions are expected to affect the conformation of loosely grafted molecules. This should strongly depend on the pH value of the solution which determines the degree of ionization. In order to study the pH responsive nature of the PAA brushes, each sample was dissolved in double distilled Milli-Q water. The solutions were heated at 60 °C overnight to aid dissolution; however, the 5% grafted brush (**P4**) never dissolved, because the hydrophobic contribution from the PMMA backbone becomes substantial. In order to minimize clustering and observe single molecule behavior, the solutions

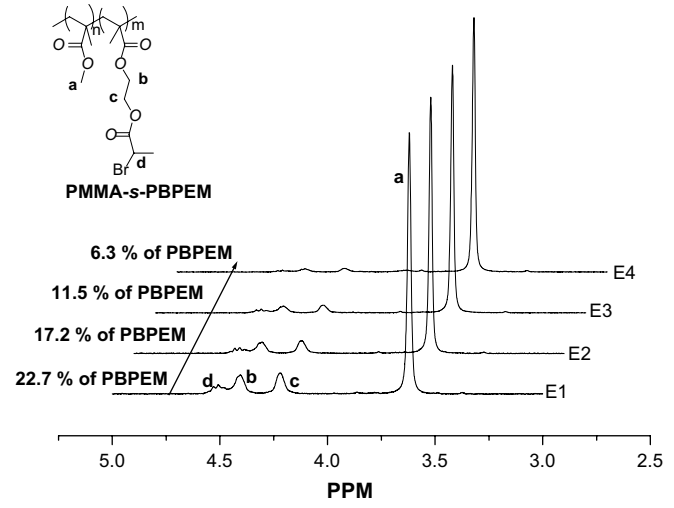

Fig. 2. ^{1}H NMR spectra of PMMA-*s*-PBPEM (**E1**, **E2**, **E3** and **E4**) with different amounts of the initiating groups along the backbone.

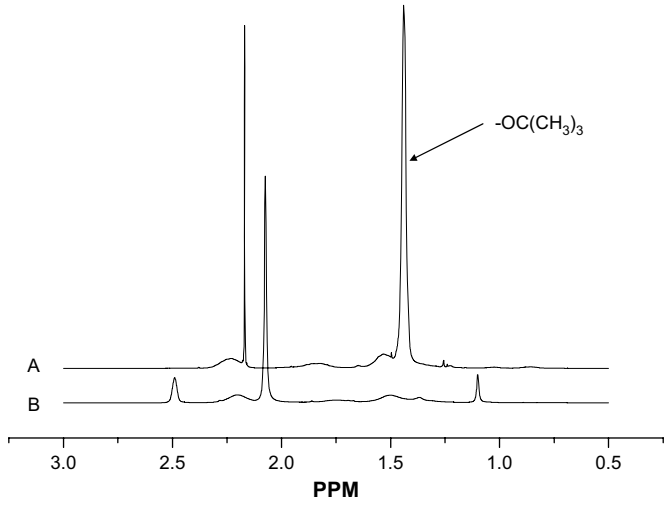

Fig. 3. ^{1}H NMR spectra of (A) **B1**, [PMMA-*s*-(PBPEM-*g*-PtBA)] and (B) **P1**, [PMMA-*s*-(PBPEM-*g*-PAA)].

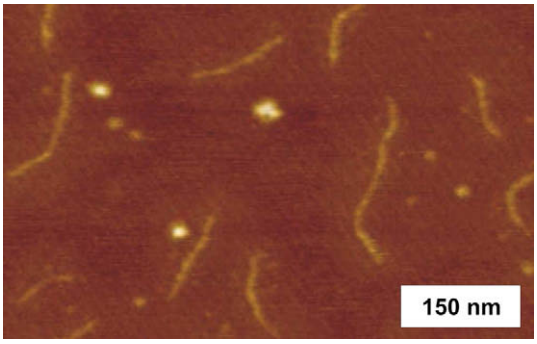

Fig. 4. Molecular imaging by AFM shows single molecules of 100%-grafted PAA brushes (**P0**) adsorbed on mica from aqueous (pH = 3.8) solution. The molecules demonstrate extended conformation with all-*trans* backbone which gives the length per monomeric unit of $l_m \cong 0.24$ nm.

were diluted to 0.05 mg/mL. After adjusting the pH and allowing some time for equilibration, the solutions were spin cast onto mica and imaged by AFM. The AFM results for the 10% (**P3**) and 20% (**P1**) grafted samples are reported in Figs. 5 and 6. As seen in the height images, each brush molecule made a gradual transition from a compact globule to an extended conformation. At low pH almost all AA groups are protonated, so repulsion between side chains is minimal. This allows the PMMA backbone to coil and results in the compact collapsed molecules observed. As the pH is increased and AA groups begin to deprotonate, the repulsion between side chains increases forcing the backbone to unfold. At the highest pH the side chains are almost fully deprotonated and repel strongly enough to extend the backbone. How quickly the transition occurs is dependent on the grafting density, the more densely grafted brush becoming extended at a slightly lower pH than the more loosely grafted brush. The onset of expansion for **P1** (20% grafting) was observed at pH ≅ 6 (Fig. 6). This is consistent with the literature data available for linear PAA. At pH larger than the effective p*K*a of AA units in a polymer, most of the monomers are ionized resulting in extension of the PAA chains. At lower pH values, the carboxylic groups become protonated, i.e. uncharged, resulting in molecular collapse to a globular conformation [62]. The effective p*K* depends on molecular weight and ranges within 6.8–7 for molecular weights of order 100 kDa. One also expects that p*K* will slightly increase with the grafting density, since branched polymers have lower degree of ionization than linear chains due to higher local concentration of ionized monomers and their counterions [63]. There is also a complex effect of a charged substrate [56], which is not covered by this study.

To follow the observed transition quantitatively, AFM images were analyzed for molecular areas, the results of which are shown in the graphs in Fig. 5. At low pH (pH < 7) the molecules are compact and have the smallest average area (~200 nm^2 for **P3**). Raising pH leads to unfolding of the polymers and the increase of the average area up to >600 nm^2 for **P3**. As would be expected, the more loosely grafted 10% brush (**P3**) has smaller areas than the more densely grafted 20% brush (**P1**). However, quantitative

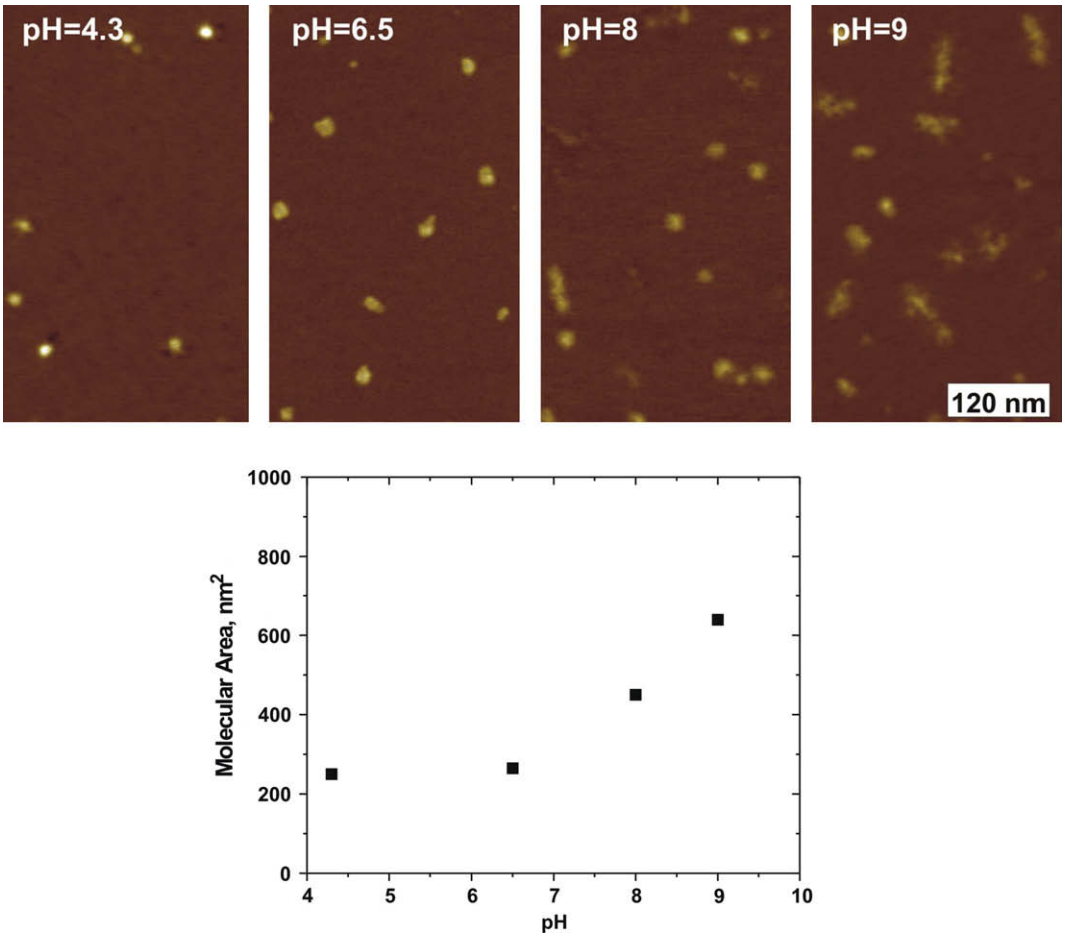

Fig. 5. The 10% grafted PAA brush (**P3**) gradually unfolded as the solution pH increased, as is seen by AFM height images. This transition was quantified by analyzing the images for molecular area.

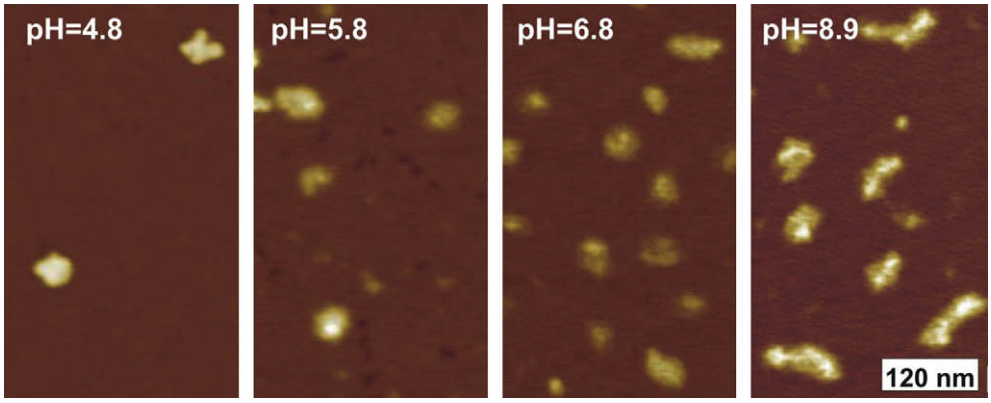

Fig. 6. The 20% graft PAA brush (**P1**) behaves very similarly to the 10% brush (**P3**), going from a compact globule to an extended molecule with an increase in pH. At lower pH values, one observes large particles that are attributed to molecular aggregates at the poor solvent conditions.

analysis of the **P1** (20%) images was inaccurate due to molecular aggregation at low pH values.

The molecular aggregation was confirmed by dynamic light scattering which was used to measure the apparent hydrodynamic diameters of **P1**, **P2** and **P3** as a function of pH. First, the samples were prepared from solutions with the same concentrations (0.05 mg/mL) as those employed for AFM investigations. At this low concentration, there was an inherent problem with DLS measurement. Since the brush molecules are very small due to low grafting densities, they approached the detection limit for DLS (~ 10 nm) as well as the limit in scattering intensity detection. For samples measured from a higher concentration solution (0.3 mg/mL), as shown in Fig. 7, two trends were observed. The apparent diameter of **P1** was about 160 nm at pH 5.4, which can be explained by intermolecular aggregation due to hydrophobic interactions. Upon increase of pH, there was a significant decrease in the hydrodynamic diameter of the molecules, which indicates that acrylic acid groups became ionized and intermolecular aggregation was slowly disrupted. On the other hand, while the same general trend was observed for **P2** and **P3**, the decrease in the hydrodynamic diameter was relatively smaller. When compared with **P1**, there are more hydrophobic contributions from the PMMA backbone for the more loosely grafted brushes, **P2** and **P3**, which might not be able to be overcome by the deprotonation of AA groups enough to disturb aggregation. Similar observations were recently reported for temperature sensitive molecular brushes [64–66].

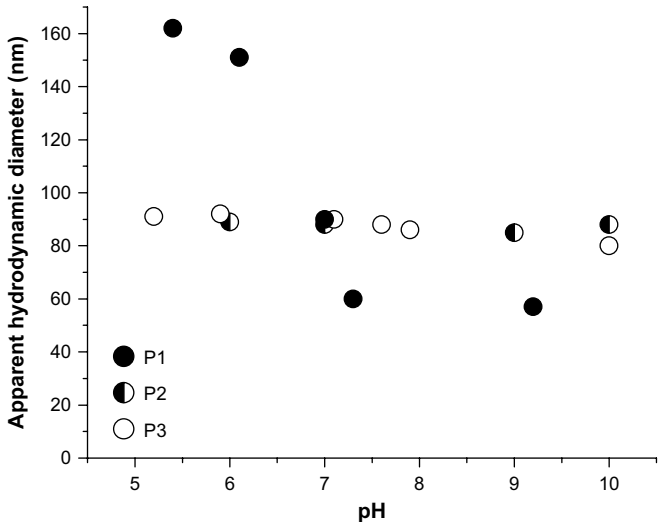

Fig. 7. Apparent hydrodynamic diameters **P1** (20% grafting density), **P2** (15% grafting density) and **P3** (10% grafting density) as a function of pH (0.3 mg/mL).

4. Conclusions

ATRP "grafting from" approach was employed to prepare a series of molecular brushes with loosely grafted PAA side chains. Well-defined PMMA-*stat*-PHEMATMS copolymers with four different compositions along the backbone (PMMA/PHEMATMS = 80/20, 85/15, 90/10 and 95/5) were synthesized by ATRP. After transformation of PHEMATMS to bromopropionyl ATRP initiating groups, PBPEM, molecular brushes with PtBA side chains were synthesized from these macroinitiators, followed by hydrolysis of the PtBA chains, leading to PAA brushes. Copolymer backbones and resulting molecular brushes were characterized by GPC and ^{1}H NMR spectroscopy. Based on the results of AFM studies, we demonstrate that the loosely grafted PAA brushes undergo a globule-to-extended conformational transition in aqueous solution in response to increashing pH. The conformational behavior was compared with 100%-grafted PAA brushes. Unlike the loose brushes, the 100%-grafted molecules demonstrated fully extended conformation in a broad range of pH values (pH = 2–9) due to steric repulsion of the densely grafted side chains which is significantly enhanced upon adsorption to the substrate.

Acknowledgements

This work was financially supported by the National Science Foundation (ECS 01-03307 and DMR 05-49353).

References

[1] Neugebauer D, Zhang Y, Pakula T, Sheiko SS, Matyjaszewski K. Macromolecules 2003;36:6746–55.
[2] Pakula T, Zhang Y, Matyjaszewski K, Lee H-i, Boerner H, Qin S, et al. Polymer 2006;47:7198–206.
[3] Djalali R, Li S-Y, Schmidt M. Macromolecules 2002;35:4282–8.
[4] Zhang M, Estournes C, Bietsch W, Mueller AHE. Adv Funct Mater 2004;14:871–82.
[5] Zhang M, Teissier P, Krekhova M, Cabuil V, Mueller AHE. Prog Colloid Polym Sci 2004;126:35–9.
[6] Fischer K, Schmidt M. Macromol Rapid Commun 2001;22:787–91.
[7] Hardingham TE, Perkins SJ, Muir H. Biochem Soc Trans 1983;11:128–30.
[8] Muir H. Biochem Soc Trans 1983;11:613–22.
[9] Simon WH. J Biomech 1971;4:379–89.
[10] Jay GD. Connect Tissue Res 1992;28:71–88.
[11] Scott JE. Biochemistry 1996;35:8795–9.
[12] Kaneider NC, Dunzendorfer S, Wiedermann CJ. Biochemistry 2004;43:237–44.
[13] Khalsa PS, Eisenberg SR. J Biomech 1997;30:589–94.
[14] Seog J, Dean D, Plaas AHK, Wong-Palms S, Grodzinsky AJ, Ortiz C. Macromolecules 2002;35:5601–15.

[15] Chen L, Yang BL, Wu Y, Yee A, Yang BB. Biochemistry 2003;42:8332–41.
[16] Li Z, Hou W-S, Broemme D. Biochemistry 2000;39:529–36.
[17] Lienkamp K, Noe L, Breniaux M-H, Lieberwirth I, Groehn F, Wegner G. Macromolecules 2007;40:2486–502.
[18] Chaterji S, Kwon IK, Park K. Prog Polym Sci 2007;32:1083–122.
[19] Dimitrov I, Trzebicka B, Mueller AHE, Dworak A, Tsvetanov CB. Prog Polym Sci 2007;32:1275–343.
[20] Hoffman AS, Stayton PS. Prog Polym Sci 2007;32:922–32.
[21] Kumar A, Srivastava A, Galaev IY, Mattiasson B. Prog Polym Sci 2007;32:1205–37.
[22] Rapoport N. Prog Polym Sci 2007;32:962–90.
[23] Yagci Y, Tasdelen MA. Prog Polym Sci 2006;31:1133–70.
[24] Yamato M, Akiyama Y, Kobayashi J, Yang J, Kikuchi A, Okano T. Prog Polym Sci 2007;32:1123–33.
[25] Braunecker WA, Matyjaszewski K. Prog Polym Sci 2007;32:93–146.
[26] Tsarevsky NV, Matyjaszewski K, Xia J. Chem Rev 2007;107:2270–99.
[27] Matyjaszewski K. J Phys Org Chem 1995;8:197–207.
[28] Matyjaszewski K. Prog Polym Sci 2005;30:858–75.
[29] Matyjaszewski K, Gnanou Y, Leibler L, editors. Macromolecular engineering: from precise macromolecular synthesis to macroscopic materials properties and applications. Weinheim: Wiley-VCH; 2007.
[30] Matyjaszewski K, Xia J. Chem Rev 2001;101:2921–90.
[31] Wang J-S, Matyjaszewski K. J Am Chem Soc 1995;117:5614–5.
[32] Zhang M, Mueller AHE. J Polym Sci Part A Polym Chem 2005;43:3461–81.
[33] Ishizu K. Polym. J 2004;36:775–92.
[34] Ishizu K, Satoh J, Sogabe A. J Colloid Interface Sci 2004;274:472–9.
[35] Ishizu K, Yamada H. Macromolecules 2007;40:3056–61.
[36] Vogt AP, Sumerlin BS. Macromolecules 2006;39:5286–92.
[37] Beers KL, Gaynor SG, Matyjaszewski K, Sheiko SS, Moeller M. Macromolecules 1998;31:9413–5.
[38] Sheiko SS, Sumerlin BS, Matyjaszewski K. Prog Polym Sci 2008;33:759–85.
[39] Gu L, Shen Z, Zhang S, Lu G, Zhang X, Huang X. Macromolecules 2007;40:4486–93.
[40] Peng D, Zhang X, Huang X. Polymer 2006;47:6072–80.
[41] Matyjaszewski K, Qin S, Boyce JR, Shirvanyants D, Sheiko SS. Macromolecules 2003;36:1843–9.
[42] Boyce JR, Shirvanyants D, Sheiko SS, Ivanov DA, Qin S, Boerner H, et al. Langmuir 2004;20:6005–11.
[43] Peng D, Zhang X, Huang X. Macromolecules 2006;39:4945–7.
[44] Peng D, Feng C, Lu G, Zhang S, Zhang X, Huang X. J Polym Sci Part A Polym Chem 2007;45:3687–97.
[45] Khelfallah N, Gunari N, Fischer K, Gkogkas G, Hadjichristidis N, Schmidt M. Macromol Rapid Commun 2005;26:1693–7.
[46] Boerner HG, Beers K, Matyjaszewski K, Sheiko SS, Moeller M. Macromolecules 2001;34:4375–83.
[47] Lee H, Jakubowski W, Matyjaszewski K, Yu S, Sheiko SS. Macromolecules 2006;39:4983–9.
[48] Zhang M, Breiner T, Mori H, Muller AHE. Polymer 2003;44:1449–58.
[49] Cheng G, Boeker A, Zhang M, Krausch G, Mueller AHE. Macromolecules 2001;34:6883–8.
[50] Qin S, Saget J, Pyun J, Jia S, Kowalewski T, Matyjaszewski K. Macromolecules 2003;36:8969–77.
[51] Lee H-i, Matyjaszewski K, Yu S, Sheiko SS. Macromolecules 2005;38:8264–71.
[52] Lord SJ, Sheiko SS, LaRue I, Lee H-I, Matyjaszewski K. Macromolecules 2004;37:4235–40.
[53] Boerner HG, Duran D, Matyjaszewski K, da Silva M, Sheiko SS. Macromolecules 2002;35:3387–94.
[54] Currie EPK, Sieval AB, Avena M, Zuilhof H, Sudhoelter EJR, Stuart MAC. Langmuir 1999;15:7116–8.
[55] Laguecir A, Ulrich S, Labille J, Fatin-Rouge N, Stoll S, Buffle J. Eur Polym J 2006;42:1135–44.
[56] Sonnenberg L, Parvole J, Borisov O, Billon L, Gaub HE, Seitz M. Macromolecules 2006;39:281–8.
[57] Sheiko SS, Prokhorova SA, Beers KL, Matyjaszewski K, Potemkin II, Khokhlov AR, et al. Macromolecules 2001;34:8354–60.
[58] Potemkin II, Khokhlov AR, Prokhorova S, Sheiko SS, Moeller M, Beers KL, et al. Macromolecules 2004;37:3918–23.
[59] Sun F, Sheiko SS, Moeller M, Beers K, Matyjaszewski K. J Phys Chem A 2004;108:9682–6.
[60] Boyce JR, Sheiko SS, Neugebauer D, Matyjaszewski K. Polym Mater Sci Eng Prepr 2006;94:253–4.
[61] Sheiko SS, Sun FC, Randall A, Shirvanyants D, Rubinstein M, Lee H-i, et al. Nature 2006;440:191–4.
[62] Raphael E, Joanny JF. Europhys Lett 1990;13:623–8.
[63] Plamper FA, Becker H, Lanzendoerfer M, Patel M, Wittemann A, Ballauff M, et al. Macromol Chem Phys 2005;206:1813–25.
[64] Pietrasik J, Sumerlin BS, Lee RY, Matyjaszewski K. Macromol Chem Phys 2007;208:30–6.
[65] Lee H-i, Pietrasik J, Matyjaszewski K. Macromolecules 2006;39:3914–20.
[66] Yamamoto S-i, Pietrasik J, Matyjaszewski K. Macromolecules 2007;40:9348–53.